AN OPTIMIZED EMISSIVITY AND TEMPERATURE SEPARATION FROM HYPERSPECTRAL THERMAL INFRARED DATA

Yang Hang, Zhang Lifu, Tong Qingxi, Cheng Xiaoyun
State Key Laboratory of Remote Sensing Science, Institute of Remote Sensing Applications, Chinese Academy of Sciences, Beijing, 100101

KEY WORDS: Airborne Hyperspectral Thermal Infrared Data; Temperature and Emissivity separation; Noise Departure; ISSTES algorithm; Aster_TES algorithm

ABSTRACT: This paper introduces the noise term to the radiative transfer equation. The noise appears to be amplified when the atmospheric correction. After researching the algorithms of Aster_TES and ISSTES based on TASI dataset, the results show that: the accuracy of temperature and emissivity retrieved from improved algorithm is higher than the other two; the images by Aster_tes have better definition on space dimension. These results have important practical value on the temperature and emissivity separation from low emissivity surfaces, such as mental and some man-made surfaces.

INTRODUCTION

The temperature and emissivity separation is a quite attractive and challenging objective for many quantitative remote sensing applications. Surface temperature and emissivity are critical parameters in the land surface process. From the radiative transfer model, land surface temperature and emissivity are coupled, and the retrieval of land surface temperature and emissivity represents an ill-posed problem because of solving N+1 unknown with N equations. Presently, more and more researchers dedicate to the research on temperature and emissivity separation, and raise many important methods (Anne B,1980; Gillespie, A R,1985; Kealy P S, 1990; Matsunaga T A, 1992; Borel C C, 1998; Gillespie A R, 1998; Watson, K. , 1992; Wang, X., et al, 2009.).

This paper puts forward a new idea to separate the temperature and emissivity: introducing the noise term into the radiative transfer equation. After removing the noises by moving average method, the result of TES not only keep the shape and the smoothness of emissivity spectra but reducing the transfer noise to temperature and emissivity. Lastly, we compute the RSME between the computed surface radiance and measured surface radiance using the emissivity and temperature removed noises.

1.METHOLDOLOGY

1.1 Traditional radiative transfer theory

It is assumed that the atmospheric effect was removed or the radiance was measured on ground. Based on Kirchholff law, ground-leaving radiance can be written as:

$$L_{s,i} = \varepsilon_i B_i(T_s) + (1-\varepsilon_i) L_{atm\downarrow,i} \quad (1)$$

Where, $L_{s,i}$ is ground-leaving radiance of channel *i* measured by TASI sensor; ε_i is surface emissivity of channel *i*; $B_i(T_s)$ is the Plank radiance at surface temperature; $L_{atm\downarrow,i}$ is the down-welling sky radiance.

According to the studied region, the up-welling path radiance, the down-welling sky radiance (Fig.1), and the atmospheric transmittance (Fig.2) consisting with the TASI are obtained by the MODTRAN software.

Therefore, if the objective optimal temperature was obtained, objective emissivity can be calculated by the following equation:

$$\varepsilon_i = \frac{L_{s,i} - L_{atm\downarrow,i}}{B_i(T_s) - L_{atm\downarrow,i}} \qquad (2)$$

Where, $L_{s,i} = (L_i - L_{atm\uparrow,i})/\tau_i$

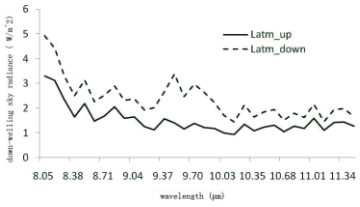

Fig.1. The up-welling path radiance and down-welling sky radiance by the MODTRAN for TASI data

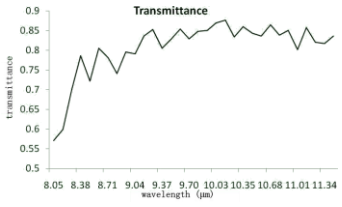

Fig.2. The atmospheric transmittance by the MODTRAN software for TASI data

1.2 Aster algorithm

Gillespie, et al.(1998) developed a new algorithm of temperature and emissivity separation. The TES method is composed by three basic modules: NEM, Ratio, MMD.

NEM module (normalized emissivity method): to begin, the emissivity of each channel is assumed to be 0.97, in order to calculate a temperature and the other emissivities. These emissivities permit iterative correction for removing the effect of down-welling sky irradiance, and then an initial surface temperature T_s^0 can be estimated.

Ratio module: the relative spectral would be calculated by the equation (3). It is an important advantage of the method that the emissivity spectral shape would be kept during the process of iteration.

$$\beta_i = \frac{\varepsilon_i}{\overline{\varepsilon}} = \frac{L_i / B_i(T_s^0)}{(\frac{1}{N}\sum_{i=1}^{N} L_i) / (\frac{1}{N}\sum_{i=1}^{N} B_i(T_s^0))} \qquad (3)$$

Where, L_i is the radiance of channel *i* after atmospheric correction; T_s^0 is the initial temperature calculated by the NEM module; ε_i is surface emissivity of channel *i*; $\overline{\varepsilon}$ is the average emissivity; *N* is the number of bands, for TASI data, *N*=32.

MMD module: the empirical relationship between $\varepsilon_{\min}$ and MMD, where MMD = max(β) - min(β) is a key feature of the TES algorithm. The $\varepsilon_{\min}$ is calculated by the empirical relationship (eq.4)

$$\varepsilon_{\min} = a - b * MMD^c \qquad (4)$$

Where, *a*, *b*, and *c* is the coefficient which depend on the analysis of laboratory emissivity spectra, and vary with different sensors. In order to raising the accuracy, it is essential to build a new empirical relationship between $\varepsilon_{\min}$ and MMD based on the TASI band setting:

$$\varepsilon_{\min} = 0.9924 - 0.9174 \times MMD^{0.9723} \qquad (r^2 = 0.988, SD = 0.0156) \qquad (5)$$

1.3 ISSTES algorithm

ISSTES method was first described by Borel. The algorithm's basis is the assumption that the surface emissivity is smoother than the atmospheric downward radiance. Given the definition of smoothness for emissivity curves, such as second difference (eq.6), one can calculated the smoothness of the family of emissivity curves correspond to different temperature. The optimal surface temperature corresponds to the smoothest emissivity curve, in which the atmospheric absorption lines disappear. And then the surface emissivity can be calculated by thermal infrared radiation transfer equation:

$$s_n = \sum_{i=2}^{N} (\varepsilon_{i-1} - 2\varepsilon_i + \varepsilon_{i+1})^2 \quad (n=2,3\ldots\ldots,N-1) \tag{6}$$

where, N is the band number. This method is sensitivity to noises: when there are no noises, it is easy to confirm the optimal emissivity curve and corresponding temperature (Fig.3); when there are noises, the smoothness indices of emissivity curves change slowly on the both sides of the minimum, which causes the temperature error increasing (Fig.4).

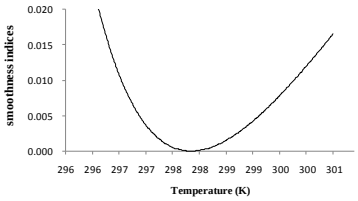

Fig.3. smoothness indices of emissivity curves change with temperature change without noise

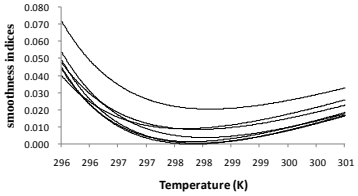

Fig.4. smoothness indices of emissivity curves change with temperature change under difference noise level

1.4 Improved algorithm based on noise Separation

Theoritical basis of improved algorithm

According to the radiance transfer equation, thermal radiance received by sensors can be written as:

$$L_i = \tau_i \varepsilon_i B_i(T_s) + \tau_i (1-\varepsilon_i) L_{atm\downarrow,i} + L_{atm\uparrow,i} \tag{7}$$

In fact, this equation is not closed, because that the radiance recorded by sensors include different noises (noted as N), such as the sensor added noise, pixel proximity effect, and the uncertainties of atmospheric parameters. Therefore, the equation 3 can be written as:

$$L_i = \tau_i \varepsilon_i B_i(T_s) + \tau_i (1-\varepsilon_i) L_{atm\downarrow,i} + L_{atm\uparrow,i} + N \tag{8}$$

If let $L_{s,i} = \varepsilon_i B_i(T_s) + (1-\varepsilon_i) L_{atm\downarrow,i}$, then

$$L_{s,i} = \frac{L_i - L_{atm\uparrow,i}}{\tau_i} - \frac{N}{\tau_i} \tag{9}$$

From equation 9, we can know noise will be amplified after atmospheric correction. Therefore, equation 2 can be modified as:

$$\varepsilon_i = \frac{L_{s,i} - L_{atm\downarrow,i}}{B_i(T_s) - L_{atm\downarrow,i}} + \frac{N}{\tau(B_i(T_s) - L_{atm\downarrow,i})} \tag{10}$$

But, it is difficult to get the real noises. In this paper, emissivity was calculate by equation 2, and then noises were removed using moving average method (R. C. Gonzalez, 2008). $\varepsilon_n^{'}$ which indicates removing-noises emissivity was substituted into equation 1 and then $L_{s,i}^{'}$ was gotten. Therefore, cost function can be written as:

$$E^2 = \sum_n (L_{s,i} - L_{s,i}^{'})^2 \tag{11}$$

$L_{s,i}$ is atmospheric-corrected surface radiance. The emissivity and temperature corresponding to the

minimum of E^2 is the optimal result.

Algorithm flow

S1.Esimating pixel initialization temperature (T_ini): compute the radiance temperature of all bands, and select the max temperature as pixel initialization temperature;

S2.Set the temperature step (T_{step}) to 1K.

S3.Compute the emissivities using equation 2;

S4.emissivity filter;

S5.compute the ground-leaving radiance using filtered emissivity and temperature.

S6.compute RMSE (cost function), and set the stopping condition of program. If the error decreased, let $T=T+T_{step,}$ and then Repeat step 3; if T_{step} satisfies the ending condition, then end program, if T_{step} doesn't satisfies the ending condition, then run step 7.

S7. Let Tstep = -Tstep/2，T=T+Tstep。Repeat step 3。

2.STUDY MATERIALS AND DATA PROCESSING

Evaluation of retrieval accuracy is an important task for practical application. In this paper, the field data was used to analyze the retrieval accuracy from the two sides of temperature and emissivity.

The experiment data is important to validate and test the algorithms developed for temperature and emissivity separation using the thermal airborne hyperspectral imager. The aircraft images and the in situ data were acquired simultaneously in the framework of field campaigns at Shijiazhuang, Hebei province in 2010. The fly region lies in 38°0'10" ~38°6'20"N,114°26'34.01"~114°30'0.01"E, with 30 km in north-south, and 5.03 km in east-west, covering an area of 57.34 km^2. The aircraft campaign was conducted from July 25, 2010 to August 15, 2010, and three time phase (morning, noon, evening), two heights (0.5 km and 1 km) images of TASI were acquired.

In the field campaign, the typical surface temperature and emissivity were measured in step with the airborne campaign. The temperature measurement time was within 5 minutes before or after the covering time for plane. For each sample pixel, about 20-30 temperature values were read uniformity, whose average was calculated to represent the true temperature for the sample pixel, and the longitude-latitude coordinates were also recorded. Temperature measurements were conducted using different broadband and multiband field thermal radiometers. MINOLTA/LAND infrared thermometer will response to broadband radiometers, while model CIMEL CE312 is multiband radiometer. The accuracy of the two instruments is about 0.1 K. Field measurements include road (cement and asphaltum), crop (maze, pachyrhizus and peanut), building roof, water, and plaza etc. These measured data were used to precision analysis of temperature and emissivity separation.

3.RESULT AND DISCUSSION

3.1 Analysis of Temperature Accuracy

Before the analysis of temperature accuracy, it is necessity to calibrate the infrared temperature into true temperature which is equivalent to be measured by mercury thermometer. The spatial resolution of TASI images is 0.59 m when the flying height is 0.5 km, and the spatial resolution of TASI images is 1.19 m when the flying height is 1 km. Therefore, it is easy to locate the pixel in the TASI image according to the latitude and longitude coordinates recorded during the field campaign, and compare the retrieved temperature with the measured temperature (Table 1).

As shown in Table 2, the temperature deviations of improved algorithm is the minimum (1.49K), and standard deviations is 0.89K. The temperature deviations of ISSTES algorithm is the second minimum (1.58K), and standard deviations is 1.04K. The temperature deviations of Aster_tes algorithm is the

maximum (1.78K), and standard deviations is 1.17K. Therefore, improved algorithm can improve precision of temperature.

Table 1. Comparison of retrieved temperature and field-measured temperature for samples

Surface type	True T /K	Temperature bias		
		Aster_TES	NSTES	ISSTES
Cement road 1	316.23	3.07	0.35	1.50
Water in park1	303.78	1.44	1.90	2.37
White cloth	307.90	2.10	1.43	0.74
Black cloth	311.18	3.90	0.73	0.29
Grass in field	303.98	1.03	0.73	0.77
Cement road 2	303.98	2.45	2.51	2.91
Lianqiang residential roof	304.40	0.30	0.27	0.02
Cement plaza	304.98	1.27	1.40	1.75
Bolin residential roof	302.57	3.80	3.41	3.74
Maze	295.71	1.95	2.63	2.60
Granite pavement in park	297.08	0.33	1.41	1.30
Water in park2	299.33	0.87	1.65	1.68
Grass in park	295.84	0.86	1.32	1.16
River-water	299.15	1.56	1.12	1.24
mean of T deviation		1.78	1.49	1.58
STD of T deviation		1.17	0.89	1.04

3.2 Analysis of Emissivity Accuracy

As hyperspectral data of TASI, it is necessary to further analyze the difference between the retrieved emissivity spectrum and the true values.

Fig.5 is the comparison of retrieved emissivity and lib-acquired emissivity. The result shows that emissivity of improved algorithm is similar to that of ISSTES algorithm, and there is obvious difference from Aster_tes algorithm and the other two algorithms. But the emissivity cure shapes retrieved by the three algorithms are very similar.Fig.6 is the false-color images of bands 32 (R), 22(G), 11(B) for TASI data, which are retrieved by above three methods. The result shows that the image retrieved by Aster_TES algorithm is more definitional and better for object identification.

Fig.5. Comparison of retrieved emissivity and lib-acquired emissivity

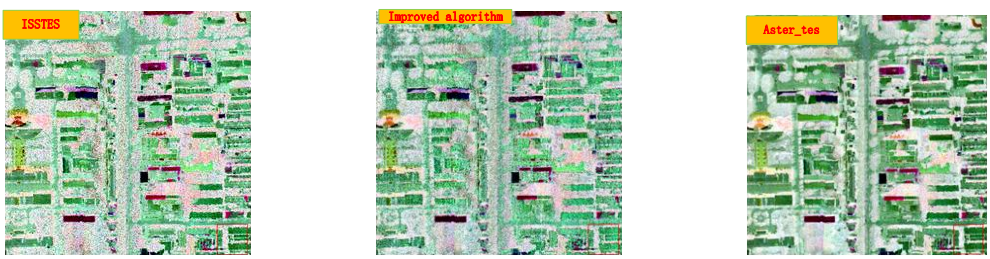

Fig.6. The False-color images of bands 32 (R), 22(G), 11(B) for TASI data

4.CONCLUSIONS

This paper proposes an improved temperature and emissivity separation algorithm based on noise separation. The research results show that improved algorithm can improve precision of temperature, but the Aster_tes has better definition on space dimension. The main reason may be that the noise of measurement data is very complexity, and it is difficult to remove the noise by only one method.

In a word, improved algorithm improves the temperature accuracy by noise removing and iterative algorithm. This method will be effective for man-made surface, metal mineral et.al. On the other hand, improved method will be obtained better accuracy if MMD algorithm is introduced to correct emissivity, which is the next work in the future.

ACKNOWLEDGEMENTS

This work is sponsored by a grant from national natural Science foundation (30772890, 41072248) and he National High Technology Research and Development Program of China(863 Program, 2008AA121102, 2008AA121103).

REFERENCES

[1] Anne B. Kahle, Daryl P. Madura, and James M. Soha, 1980. Middle infrared multispectral aircraft scanner data: analysis for geological applications[J]. Applied Optics, 19(14):2279-2290

[2] Borel C C, 1998. Surface emissivity and temperature retrieval for a hyperspectral sensor[A]. Proceedings of the International Geoscience and Remote Sensing Symposium[C], 1: 546-549.

[3] Gillespie, A R,1985. Lithologic mapping of silicate rocks using TIMS[A]. The TIMS Data User's Workshop, JPL Propulsion Laboratory[C]. Passadena, CA.

[4] Gillespie A R, Matsunaga T, Rokugawa S, et al, 1998. A temperature and emissivity separation algorithm for advanced spaceborne thermal emission and reflection radiometer(ASTER) images [J]. IEEE Trans. Geosci. Remote Sens., 36(4):1113-1126.

[5] Kealy P S, Gabell A R, 1990. Estimation of emissivity and temperature using alpha coefficients [C]. Proceedings of the Second TIMS Workshop. Pasadena, CA: Jet Propulsion Laboratory, JPL Publication 90-55, 11-15.

[6] Matsunaga T A, 1992. A temperature-emissivity separation method using an empirical relationship between the mean, the maximum and the minimum of the thermal infrared emissivity spectrum [J]. Journal of Remote Sensing Society of Japan,42: 83-106.

[7] R. C. Gonzalez, R. E. Woods, S. L. Eddins. 2008. Digital Image Processing Using Matlab. Beijing, Publishing House of Electronics Industry.

[8] Schmugge T.Hook S J.Coll C. Recovering surface temperature and emissivity from thermal infrared multispectral data. Remote Sensing of Enironment. 65:121-131.

[9] Sobrino, J., V. Caselles, and C. Coll, 1993, Theoretical split-window algorithms for determining the actual surface temperature. Il Nuovo Cimento C. 16(3): p. 219-236.

[10] Wang, X., et al, 2009. A new method for temperature/emissivity separation from hyperspectral thermal infrared data[J]: IEEE.

[11] Watson, K. , 1992. Spectral ratio method for measuring emissivity[J]. Remote Sensing of Environment. 42(2): 113-116.

[12] Yang Hang, Zhang Lifu, Fang Junyong et.al,2010. Algorithm Research of Building Materials Emissivity Extracting. IGARSS 2010